Desalination and Water Treatment
www.deswater.com
doi: 10.1080/19443994.2015.1098573

57 (2016) 19344–19356
September

Taylor & Francis
Taylor & Francis Group

Decolorization kinetics of Acid Blue 161 by solid peroxides catalyzed by iron in aqueous solution

Alam G. Trovó[a], Pavels Senivs[b], Ülar Palmiste[b], Mika Sillanpää[c], Walter Z. Tang[b,*]

[a]*Instituto de Química, Universidade Federal de Uberlândia, Uberlândia—MG 38400-902, Brasil, email: alamtrovo@iqufu.ufu.br*
[b]*Department of Civil and Environmental Engineering, Florida International University, Miami, FL 33174, USA, emails: pavels.senivs@gmail.com (P. Senivs), ylar.palmiste@gmail.com (Ü. Palmiste), Tel. +1 305 348 3046; Fax: +1 305 348 2802; email: tangz@fiu.edu (W.Z. Tang)*
[c]*Faculty of Technology, Department of ChemTech, Lappeenranta University of Technology, 53850 Lappeenranta, Finland, email: mika.sillanpaa@lut.fi*

Received 24 June 2015; Accepted 16 September 2015

ABSTRACT

Decolorization of Acid Blue 161 (AB161) by solid peroxides such as CaO_2 and Na_2O_2 catalyzed by iron in aqueous solution was investigated. The effect of initial pH, concentration of H_2O_2, Fe^{2+}, and AB161 on the decolorization kinetics was investigated and compared with the results by liquid H_2O_2. The experimental results show that decolorization of AB161 follows the second-order kinetic. The second decolorization rate constants and oxidation efficiency at different initial pH, Fe^{2+}, H_2O_2, and AB161 concentration were correlated with dimensionless ratios such as H_2O_2/Fe^{2+} or H_2O_2/AB161. About two dozens of correlation equations are developed in this paper to quantify the effect of the variables on the decolorization rate constants of AB161. Among solid peroxides such as CaO_2 and Na_2O_2 and liquid H_2O_2, the optimal pH and [Fe^{2+}] are 2.5 and 5.0×10^{-4} mol L^{-1}, while the concentration of CaO_2, Na_2O_2, and H_2O_2 is 0.30, 0.25 g L^{-1} and 3.1×10^{-3} mol L^{-1}, respectively. Our experimental results show that decolorization kinetics of AB161 using liquid H_2O_2 is faster than that using CaO_2 and Na_2O_2 catalyzed by Fe^{2+}, while decolorization rate of AB161 by CaO_2 is slightly faster than that by Na_2O_2 due to the fact that the CaO_2 is a fine powder of an average diameter of 0.74 mm and Na_2O_2 is a particle with an average diameter of 1 mm. Regardless of the solid or liquid peroxide forms, e.g. CaO_2, Na_2O_2, or liquid H_2O_2, the optimal molar ratio H_2O_2/Fe^{2+} of 12 obtained experimentally agreed reasonably with the theoretical predicted value of 11. In addition, the decolorization efficiency, η, is also not affected by the form of peroxides and decreases with the H_2O_2/AB161 when H_2O_2, Fe^{2+}, and pH were fixed at 3.1×10^{-3}, 5.0×10^{-4} mol L^{-1}, and 2.5, respectively.

Keywords: Fenton; Azo dye; Advanced oxidation processes; CaO_2; Na_2O_2; Liquid H_2O_2

1. Introduction

Azo dyes are a widespread synthetic commercial dyes which are characterized by azo bond (–N=N–) of vivid color [1,2]. These dyes are highly recalcitrant compounds and resistant to natural decomposition in the ecosystem. In addition to the esthetic problems related to the color of these dyes, they strongly absorb sunlight, thus hinder the photosynthetic activity of aquatic organisms and plants [3]. Some of the azo

*Corresponding author.

dyes are mutagenic, carcinogenic, or toxic in nature. Therefore, they may pose significant environmental damage if they were discharged into water bodies without adequate treatment [4–6].

Several conventional techniques to remove azo dyes are chemical coagulation, sedimentation, or adsorption by activated carbon [7–9]. However, these processes are phase transferring technologies without actual degradation of dyes. Advanced oxidation processes (AOPs), on the other hand, have attracted a lot of attention due to their ability to destroy azo bonds of these commercial dyes [10]. The key species of oxidants in AOPs is hydroxyl radical ($HO^{\cdot}$) which is highly reactive and is able to oxidize the most recalcitrant pollutants such as azo dyes. Thermodynamically, hydroxyl radical has a high oxidation potential (E = +2.80 V) which is lower only than that of fluorine (E = +3.03 V). Kinetically, it reacts with organic pollutants such as azo dyes with diffusion controlled rates [11,12].

Among AOPs reported, Fenton process is one of the simple, effective, fast, and efficient oxidation processes [1,2]. Traditionally, liquid hydrogen peroxide was used with ferrous iron to generate $HO^{\cdot}$, while ferrous iron is oxidized to ferric iron (Eq. (1)) [13,14]. Ferric iron produced through Eq. (1) is also able to react with H_2O_2 to regenerate ferrous iron while producing peroxide radical as shown in Eq. (2). However, the reaction is three to four magnitude slower than the reaction rate of ferrous iron with H_2O_2 (Eq. (2)) [15,16]. Therefore, it contributes to much slower oxidation kinetics during the Fenton oxidation of azo dyes. As a result, two stages of oxidation kinetics are typical during Fenton oxidation of organic pollutants.

$$Fe^{2+} + H_2O_2 \rightarrow Fe^{3+} + HO^{\cdot} + HO^{-} \quad k_1 = 76\ mol^{-1}\ L\ s^{-1} \tag{1}$$

$$Fe^{3+} + H_2O_2 \rightarrow Fe^{2+} + HO_2^{\cdot} + H^{+} \quad k_2 = 10^{-3} - 10^{-2}\ mol^{-1}\ L\ s^{-1} \tag{2}$$

Fenton process usually is affected by several parameters such as concentration of iron, hydrogen peroxide, target compound, and pH. When liquid H_2O_2 is utilized, scavenging effect of hydroxyl radical by liquid H_2O_2 and iron as shown in Eqs. (3) and (4) requires the optimal molar ratio of H_2O_2/Fe^{2+} to be 11 [17].

$$HO^{\cdot} + H_2O_2 \rightarrow HO_2^{\cdot} + H_2O \quad k_3 = 2.7 \times 10^{7}\ mol^{-1}\ L\ s^{-1} \tag{3}$$

$$Fe^{2+} + HO^{\cdot} \rightarrow Fe^{3+} + HO^{-} \quad k_4 = 3 \times 10^{8}\ mol^{-1}\ L\ s^{-1} \tag{4}$$

When solid peroxide such as CaO_2 and Na_2O_2 is used, H_2O_2 has to be released from solid peroxide before Fenton reaction takes place. Since there is a time delay during the H_2O_2 releasing process, an immediate question is whether the optimal molar ratio 11 between H_2O_2 and Fe^{2+} also holds true when solid peroxide such as CaO_2 and Na_2O_2 is used as the source of H_2O_2. In other words, whether the releasing kinetics of H_2O_2 from solid peroxide into solution could shift the optimal ratio of H_2O_2/Fe^{2+} required for the most efficient oxidation of azo dye such as AB161 remains unanswered. In the past, CaO_2 was only applied to soil remediation. For example, it was reported that degradation efficiency of petroleum hydrocarbons [18] and polycyclic aromatic hydrocarbon [19] in soil by CaO_2/Fe^{2+} was better than that by liquid H_2O_2/Fe^{2+}, because *in situ* generation of H_2O_2 from solid peroxide is slow and tends to minimize inefficient parallel reactions, i.e. the scavenging of hydroxyl radicals by liquid H_2O_2 (Eq. (3)).

To our knowledge, only a few papers investigated H_2O_2 releasing kinetics of CaO_2 in aqueous solution. For example, Northup and Cassidy [20] reported gradual release of hydrogen peroxide from CaO_2 at various pH levels. According to their data, the releasing rate of hydrogen peroxide from CaO_2 was much faster at low pH than that at higher pH. However, no data have ever been reported on H_2O_2 releasing kinetics from sodium peroxide, as well as their implication as a source of H_2O_2 during the degradation of the azo dye, Acid Blue 161 (AB161), in aqueous solution. Therefore, the objectives of the current study are to investigate the influence of different solid peroxide such as CaO_2 and Na_2O_2 at different initial pH, dosage of Fe^{2+}, and AB161 concentration on the decolorization kinetics of AB161 and to compare the decolorization kinetics by solid peroxides with that by using liquid H_2O_2.

2. Experiment

2.1. Reagents

All solutions were prepared by using deionized water. The AB161 standard (Aldrich) was used as received. H_2O_2 (50% w/w) and $FeSO_4{\cdot}7H_2O$ (Fischer Scientific), CaO_2 (75% w/w; 200 mesh particle size), Na_2SO_3 and NaOH (Sigma-Aldrich), and Na_2O_2 (96% w/w; 1 mm average diameter) (Acros Organics) were used as received. Solution of ammonium

metavanadate (MP Biomedicals) was prepared at a concentration of 0.062 mol L^{-1} in 0.58 mol L^{-1} H_2SO_4 (J.T. Baker) and used for H_2O_2 quantification.

2.2. Yield of H_2O_2 from CaO_2 and Na_2O_2 dissolution

H_2O_2 releasing kinetics from CaO_2 and Na_2O_2 dissolution was investigated at pH of 3 and 8, and different concentrations of the solid peroxides ranging from 0.6 to 48 g L^{-1}, respectively. Considering the purity of the solid peroxides and the hydrolysis reactions of Eqs. (5) and (6), the theoretical concentrations of H_2O_2 to be released from CaO_2 and Na_2O_2 solid should range from 6.2×10^{-3} to 5.0×10^{-1} mol L^{-1} and from 7.4×10^{-3} to 5.9×10^{-1} mol L^{-1}, respectively.

$$CaO_{2(s)} + 2H_2O_{(aq)} \rightarrow H_2O_{2(aq)} + Ca^{2+}_{(aq)} + 2HO^{-}_{(aq)} \quad (5)$$

$$Na_2O_{2(s)} + 2H_2O_{(aq)} \rightarrow H_2O_{2(aq)} + 2Na^{+}_{(aq)} + 2HO^{-}_{(aq)} \quad (6)$$

The dissolution of CaO_2 and Na_2O_2 increases the solution pH due to continuously releasing HO^- (Eqs. (5) and (6)). Therefore, the pH was adjusted to the initial desired value by using either H_2SO_4 or NaOH with concentrations of 9, 3 or 1 mol L^{-1}, respectively. H_2SO_4 of the same concentration was also used to maintain constant pH of the solution, while the H_2O_2 concentration in the aqueous phase was measured.

The dissolution experiments were carried out using 200 mL of deionized water (in the presence of different concentrations of the solid peroxides at different pH) in a beaker with magnetic mixing at 150 rpm. Sample aliquots (1.5 mL) were taken between 0.5 and 5 min. The samples were left at rest to separate the remaining solid peroxide powder from 0.5 to 1.0 min before ammonium metavanadate was added. Finally, a sample was taken from the supernatant to determine H_2O_2 released in the aqueous phase.

2.3. Fenton experimental procedure

Fenton experiments were carried out using 200 mL of AB161 solutions in a beaker with magnetic mixing of 150 rpm. First, the effect of pH from 2.0 to 4.0 on the decolorization kinetics of 1.0×10^{-4} mol L^{-1} AB161 was investigated with different H_2O_2 sources such as CaO_2, Na_2O_2, or liquid H_2O_2, respectively. 0.60 or 0.50 g L^{-1} of the commercial powders of CaO_2 and Na_2O_2 and 3.0×10^{-3} mol L^{-1} Fe^{2+} were used. The amount of CaO_2 and Na_2O_2 was selected to release an initial theoretical amount of H_2O_2 of 6.2×10^{-3} mol L^{-1} (Eqs. (5) and (6)). Experiments using this same amount of liquid H_2O_2 were also carried out to compare the degradation efficiency from different H_2O_2 sources. Each experiment was started by adding the desired volume of a stock solution of $FeSO_4{\cdot}7H_2O$ (0.25 mol L^{-1}) in a beaker containing a known amount of AB161. Since pH increases significantly during the dissolution of CaO_2 and Na_2O_2 due to the hydrolysis reaction of solid peroxide, the pH was adjusted using either H_2SO_4 or NaOH with concentration of 9, 3 or 1 mol L^{-1}. The H_2SO_4 or NaOH solutions were also used to keep the pH at the desired value during the Fenton experiments (Eqs. (5) and (6)). The desired amount of H_2O_2 (solid or liquid source) was added in a single step. To monitor the AB161 decolorization rate, 3 mL sample aliquots were taken between 15 s and 10 min. This sampling procedure was used for all the other experiments.

Second, under the optimal pH of 2.5 which was determined in the first step, initial concentrations of the solid peroxides of either CaO_2 or Na_2O_2 were used so that the theoretical amount of 6.2×10^{-3} mol L^{-1} H_2O_2 could be produced. Fenton experiments were carried out to investigate the effects of various Fe^{2+} concentrations ranging from 2.5×10^{-5} to 5.0×10^{-4} mol L^{-1} on the decolorization kinetics of 1.0×10^{-4} mol L^{-1} AB161 solution.

Third, at the optimal pH of 2.5 and Fe^{2+}concentration of 5.0×10^{-4} mol L^{-1}, Fenton experiments were carried out to investigate the effects of the initial concentration of CaO_2 (ranging from 0.037 to 0.88 g L^{-1}) and Na_2O_2 (ranging from 0.031 to 0.75 g L^{-1}) on the decolorization kinetics of 1.0×10^{-4} mol L^{-1} AB161. The theoretical amount of H_2O_2 produced is expected to vary from 3.8×10^{-4} to 9.2×10^{-3} mol L^{-1}. The same experiments were carried out using liquid H_2O_2 to compare the results with the decolorization kinetics of AB161 by either CaO_2 or Na_2O_2, respectively.

Fourth, under the optimal experimental conditions: pH (2.5), Fe^{2+} (5.0×10^{-4} mol L^{-1}), CaO_2 (0.30 g L^{-1}), Na_2O_2 (0.25 g L^{-1}), or liquid H_2O_2 (3.1×10^{-3} mol L^{-1}), Fenton experiments were conducted to investigate the effect of the initial AB161 concentration ranging from 1.0×10^{-4} to 1.8×10^{-4} mol L^{-1} on the decolorization kinetics of AB161.

For all the experiments, an excess of Na_2SO_3 solution (1 mol L^{-1}) was added to a sample before its analysis. The addition of overdosed Na_2SO_3 terminates the Fenton reaction by removing the residual H_2O_2 from the sample. The sample was left at rest to separate solid peroxide from the sample from 0.5 to 1.0 min before absorbance of the sample was measured.

2.4. Analytical methods

AB161 concentration during Fenton experiments was determined through the maximum absorbance measured at the wavelength (λ_{max} = 600 nm) by a pre-established calibration curve. Hydrogen peroxide was quantified spectrophotometrically as described by Nogueira et al. [21].

3. Results and discussion

3.1. H_2O_2 releasing kinetics during CaO_2 and Na_2O_2 dissolution

Fig. 1 shows that the H_2O_2 releasing kinetics during dissolution of different concentration of CaO_2 and Na_2O_2 at different initial pH.

Three major conclusions can be reached from Fig. 1. First, the dissolution rate of CaO_2 and Na_2O_2 highly depends upon initial pH. Acidic solution at pH 3 will have faster initial dissolution kinetics than basic solution at pH 8. Second, it took about two minutes to completely release H_2O_2 for both CaO_2 and Na_2O_2. And third, the H_2O_2 releasing kinetics from CaO_2 is faster than that from Na_2O_2 during the first two minutes. Since Na_2O_2 has a higher purity than CaO_2, it was assumed that Na_2O_2 would release H_2O_2 faster than CaO_2. However, when Fig. 1(a) was compared with Fig. 1(c) at 0.6, 1.2, and 6 g L^{-1}, the H_2O_2 releasing rate from CaO_2 is slightly faster than that from Na_2O_2 during the first two minutes due to different particle sizes of CaO_2 and Na_2O_2. In our experiments, CaO_2 is a fine powder with average particle size of 0.074 mm (200 mesh), which favors its dissolution due to its higher specific surface area. On the other hand, Na_2O_2 is in the form of small ball with an average diameter of about 1 mm. As a result, the specific area of CaO_2 is significantly higher than that of Na_2O_2. Therefore, the H_2O_2 releasing rate from CaO_2 is significantly faster than that from Na_2O_2 when Fig. 1(b) CaO_2 is compared with Fig. 1(d) Na_2O_2 during the first two minutes, although the same amount of H_2O_2 was observed at the end of five minutes.

H_2O_2 concentration reached a constant level after two minutes due to complete dissolution of the solid peroxide. The theoretical amount of H_2O_2 expected at pH 3 for both CaO_2 and Na_2O_2 was confirmed by measuring the H_2O_2 concentration in the aqueous solution. However, the same behavior was not

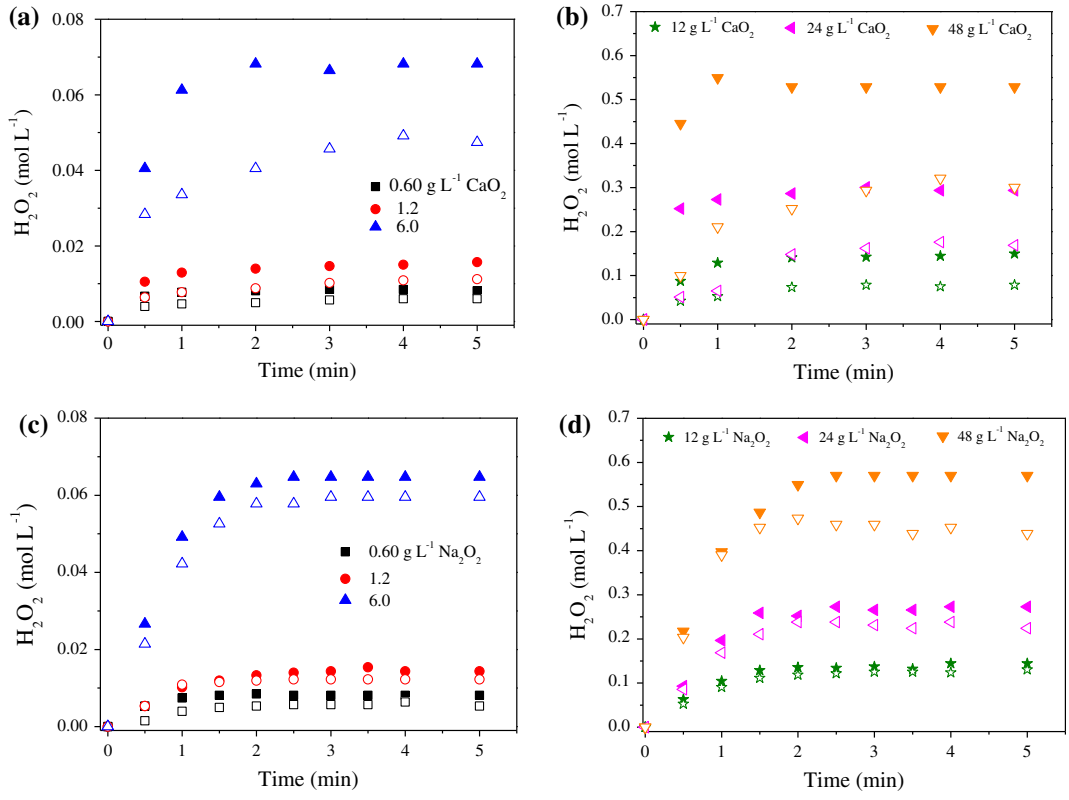

Fig. 1. H_2O_2 releasing kinetics of from CaO_2 (a and b) and Na_2O_2 (c and d) dissolution at different concentrations of the peroxide salts, at pH 3 (solid symbols) and pH 8 (open symbols).

Table 1
Second-order decolorization rate constants (k) and correlation coefficients (R^2) for each pH using different H_2O_2 sources

	CaO_2		H_2O_2		Na_2O_2	
pH	k (mol^{-1} L min^{-1})	R^2	k (mol^{-1} L min^{-1})	R^2	k (mol^{-1} L min^{-1})	R^2
2.0	3,472	0.90	3,230	0.82	3,405	0.94
2.5	4,878	0.99	12,865	0.99	4,155	0.99
3.0	2,936	0.98	4,592	0.99	1,362	0.95
3.5	199	0.96	2,588	0.96	203	0.98
4.0	91	0.99	532	0.67	76	0.74

Notes: Experimental conditions: 3.0×10^{-3} mol L^{-1} Fe^{2+}, 0.60 g L^{-1} of the commercial powder of CaO_2 (6.2×10^{-3} mol L^{-1} H_2O_2) or 0.50 g L^{-1} of Na_2O_2 (6.2×10^{-3} mol L^{-1} H_2O_2), and/or 6.2×10^{-3} mol L^{-1} of liquid H_2O_2, during Fenton decolorization of 1.0×10^{-4} mol L^{-1} AB161.

observed at higher concentrations of the solid peroxide at pH 8, because of the low stability of hydrogen peroxide in basic medium, where solid peroxides tend to decompose into water and oxygen [22]. Indeed, oxygen bubbles were observed during the dissolution experiments in basic solution. In addition, temperature increased significantly to 30˚C due to the exothermic dissolution of CaO_2 and Na_2O_2 at the higher concentrations of solid peroxide powder. The high temperature further increases decomposition of hydrogen peroxide into oxygen and water [22].

The results obtained in the present study are inconsistent with previous work reported by Northup and Cassidy [20], who reported 4 h to 6 d to completely dissolve CaO_2 at pH from 6 to 9, respectively. The major reason for this discrepancy lies in the fact that buffered solution such as $NaH_2PO_4{\cdot}H_2O$ or $Na_2HPO_4{\cdot}7H_2O$ was used in their study to keep constant pH. In our study, the buffer solution significantly decreased H_2O_2 released from CaO_2 as tested. In addition, no noticeable decolorization of AB161 by Fenton process in the presence of buffered solutions was observed. Therefore, the present work did not use the buffer solution during decolorization of AB161 by CaO_2 or Na_2O_2, because iron precipitates by phosphate [23] and prevents its reaction with H_2O_2 to produce hydroxyl radicals. For these reasons, pH was controlled by addition of either H_2SO_4 or NaOH solution.

3.2. Influence of pH

Before the effect of pH on the decolorization of AB161 is systematically assessed, kinetic models were used to quantify the effect. In the literature [24–26], different decolorization kinetic orders of dyes by Fenton process were reported. Some researchers applied the first-order kinetic model [24,25] while others used the second-order kinetic model [26]. To determine which kinetic model could best fit our experimental data, zero-, first-, and second-order kinetic models were used. The best kinetic model for all the experiments in this study is the second-order kinetics. Table 1 shows that the correlation coefficient (R^2) of the second-order kinetic model ranged from 0.90 to 0.99 at pH of 2, 2.5, 3.0, and 3.5. It also presents that correlation coefficients, R^2, for the second-order kinetic constants of CaO_2, Na_2O_2, and H_2O_2 at pH 4 decreased to 0.99, 0.74, and 0.67, respectively. Therefore, as pH increases, the degradation mechanism may have changed. Indeed, degradation kinetics of azo dye by Fenton process can be quite complex due to a great number of steps taking place simultaneously during the Fenton process [27]. For example, in the first step, ferrous ions react quickly with H_2O_2 to produce hydroxyl radical and ferric ions during the Fenton reaction, (Eq. (1)). In the second step, ferric ions can also react with H_2O_2 to generate hydroperoxide radicals (Eq. (2)), and re-produce ferrous ions, which cause the second stage degradation of the azo dye. The two-stage reactions have been confirmed by our experimental data.

Once the second-order kinetic model is selected, the effect of initial pH (ranging from 2.0 to 4.0) on the decolorization rate of AB161 by Fenton process from different sources of H_2O_2 is shown in Fig. 2. Clearly, the optimal pH is 2.5 for both the solid or liquid H_2O_2. The decolorization rates follow the order of liquid H_2O_2 > CaO_2 > Na_2O_2. When pH increased above 2.5, the decolorization rate decreases due to decreased iron solubility and less amount of H_2O_2 released from CaO_2 and Na_2O_2. On the other hand, AB161 decolorization rates decreased with the decrease in pH when the pH is below 2.5 because excessive H^+ scavenges hydroxyl radicals and form a stable oxonium ion ($H_3O_2^+$) with H_2O_2, which prevents H_2O_2 to react with iron and to generate hydroxyl radicals [17,28].

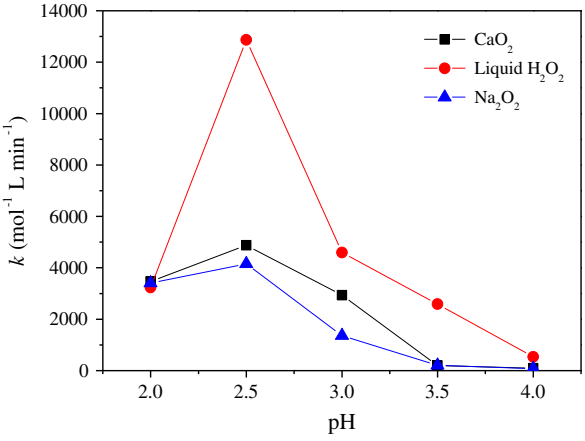

Fig. 2. Influence of pH and source of H_2O_2 on the decolorization rates of AB161 by Fenton process. Initial conditions: [AB161] = 1.0×10^{-4} mol L^{-1}; [CaO_2] and [Na_2O_2] = 0.60 and 0.50 g L^{-1}, respectively, of the commercial powders; [H_2O_2] = 6.2×10^{-3} mol L^{-1} of liquid H_2O_2.

Apparently, fast reaction between Fe^{2+} and liquid H_2O_2, in the first few seconds/minutes, is favored in the homogeneous solution such as liquid H_2O_2/Fe^{2+}. In heterogeneous systems containing either CaO_2 or Na_2O_2, H_2O_2 has to be produced *in situ* by dissolution of the peroxide solids. Since CaO_2 has a higher specific surface area than Na_2O_2, the observed decolorization rate, therefore, follows an order: liquid H_2O_2 > CaO_2 > Na_2O_2.

3.3. Influence of Fe^{2+} concentration

The influence of Fe^{2+} concentration was evaluated by fixing the initial H_2O_2 concentration at 3.0×10^{-3} mol L^{-1} and pH at 2.5. Table 2 shows that decolorization kinetics of AB161 also followed the second-order at all the Fe^{2+} concentration evaluated. The correlation between the AB161 decolorization second-order rate constants and different initial Fe^{2+} concentrations are presented in Fig. 3.

Fig. 3(a) shows that the AB161 decolorization rate constants by CaO_2 and Na_2O_2 as H_2O_2 sources increase linearly with Fe^{2+} concentration. The slopes are 1.6×10^7 and 1.3×10^7 for CaO_2 and Na_2O_2 with the same correlation coefficient R^2 of 0.99, respectively, as follows:

$$k = 1.60 \times 10^7 \times [Fe^{2+}] + 382 \quad (7)$$

$$k = 1.33 \times 10^7 \times [Fe^{2+}] + 278 \quad (8)$$

On the other hand, AB161 decolorization rate constants increased exponentially with Fe^{2+} concentration when liquid H_2O_2 was used as shown in Fig. 3(b). The regression equation (Eq. (9)) with a correlation coefficient R^2 of 0.97 is expressed as follows in Fig. 3(b):

$$\ln k = 7871 \times [Fe^{2+}] + 7.06 \quad (9)$$

As an experimental control, no AB161 decolorization was observed in the presence of 6.2×10^{-3} mol L^{-1} H_2O_2 without Fe^{2+}, which confirmed the catalytic role of Fe^{2+} in the Fenton process.

3.4. Influence of H_2O_2 concentration

The influence of H_2O_2 concentration from different sources of H_2O_2 was evaluated by fixing the initial Fe^{2+} concentration at 5.0×10^{-4} mol L^{-1} and pH at 2.5. Fig. 4 suggests that the second-order kinetic is the best model for all the H_2O_2 concentration evaluated. Table 3 presents the statistics of the correlations between the AB161 decolorization second-order rate constants and different initial concentrations of CaO_2, Na_2O_2, or liquid H_2O_2, where H_2O_2 concentration ranged from 3.8×10^{-4} to 9.2×10^{-3} mol L^{-1}.

From Fig. 4(a) and (b), three correlation equations (Eqs. (10)–(12)) between the decolorization rate constants and H_2O_2 concentration with a correlation coefficient, R^2, greater than 0.98 are obtained as follows:

$$k = 2.05 \times 10^6 \times [H_2O_2] + 277 \quad (10)$$

$$k = 1.26 \times 10^6 \times [H_2O_2] + 225 \quad (11)$$

$$k = 8.31 \times 10^6 \times [H_2O_2] - 3085 \quad (12)$$

Table 3 shows that the AB161 decolorization rate constants increase linearly with concentration of solid peroxide up to 0.30 and 0.25 g L^{-1} of CaO_2 and Na_2O_2, respectively. The theoretical amount of 3.1×10^{-3} mol L^{-1} H_2O_2 was confirmed in the experiment. When the concentration of the commercial powders of CaO_2 and Na_2O_2 was doubled to 0.60 and 0.50 g L^{-1}, respectively, theoretical amount of 6.2×10^{-3} mol L^{-1} H_2O_2 released were also experimentally confirmed. The decolorization rate constant increased but was not doubled. Fig. 4(a) shows that when concentration of CaO_2 and Na_2O_2 increased further to 0.89 and 0.75 g L^{-1} with theoretical amount of 9.2×10^{-3} mol L^{-1} H_2O_2, the decolorization rate constants of AB161 were unchanged or even decreased. On the contrary, Fig. 4(b) suggests that decolorization rate constants increase linearly with liquid H_2O_2 concentration. During the first a few minutes, Fe^{2+} reacts with

Table 2
Second-order decolorization rate constants (k) and correlation coefficients (R^2) for each Fe^{2+} concentration evaluated using different H_2O_2 sources

Fe^{2+} (mol L^{-1})	$\frac{[H_2O_2]}{[Fe^{2+}]}$	CaO_2		H_2O_2		Na_2O_2	
		k (mol^{-1} L min^{-1})	R^2	k (mol^{-1} L min^{-1})	R^2	k (mol^{-1} L min^{-1})	R^2
0	0	163	0.96	96	0.93	97	0.93
2.5×10^{-5}	2.5×10^2	600	0.99	960	0.97	407	0.99
5.0×10^{-5}	1.2×10^2	1,349	0.91	1,807	0.99	978	0.99
1.0×10^{-4}	62	2,253	0.99	3,346	0.99	1,782	0.99
2.0×10^{-4}	31	3,583	0.99	6,692	0.99	2,998	0.99
3.0×10^{-4}	21	4,878	0.99	12,865	0.99	4,155	0.99
4.0×10^{-4}	16	6,386	0.90	27,851	0.93	5,728	0.99
5.0×10^{-4}	12	8,807	0.98	51,604	0.94	6,827	0.98

Note: Experimental conditions: 0.60 g L^{-1} of the commercial powder of CaO_2 (6.2×10^{-3} mol L^{-1} H_2O_2) or 0.50 g L^{-1} of Na_2O_2 (6.2×10^{-3} mol L^{-1} H_2O_2), and/or 6.2×10^{-3} mol L^{-1} of liquid H_2O_2, during Fenton decolorization of 1.0×10^{-4} mol L^{-1} AB161 at initial pH 2.5.

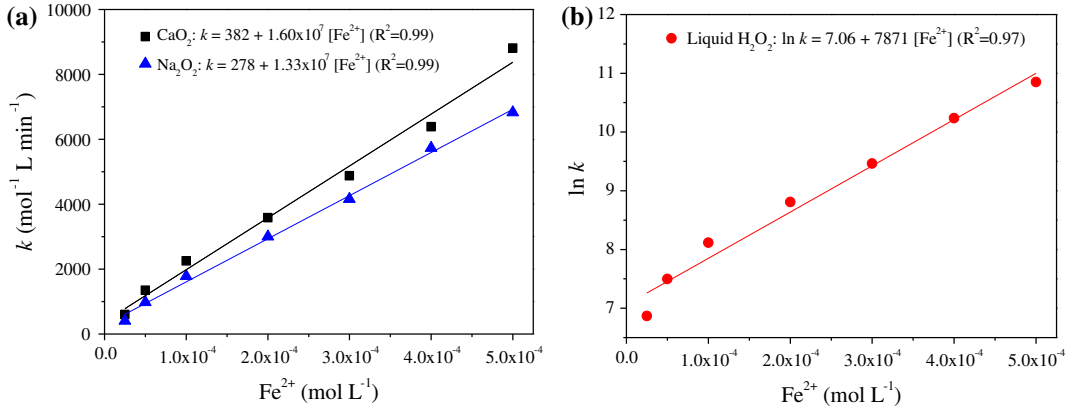

Fig. 3. (a) Linear and (b) natural logarithm correlations between the decolorization rate constants vs. Fe^{2+} concentration used, obtained during AB161 degradation by Fenton process for the different H_2O_2 sources. Initial conditions: [AB161] = 1.0×10^{-4} mol L^{-1}; [CaO_2] and [Na_2O_2] = 0.60 and 0.50 g L^{-1}, respectively, of the commercial powders; [H_2O_2] = 6.2×10^{-3} mol L^{-1} of liquid H_2O_2; pH 2.5.

H_2O_2 and leads to the rapid generation of HO·, which rapidly oxidizes and decolorizes the azo dye. The higher the concentration of H_2O_2 is, the higher concentration of hydroxyl radicals will be produced, resulting a faster decolorization of AB161. For CaO_2 and Na_2O_2, it took approximately two minutes to completely release the theoretical amount of H_2O_2 as shown in Fig. 1. As a result, the concentration of 3.1×10^{-3} mol L^{-1} H_2O_2 was chosen as the optimal condition and was used to evaluate the effects of AB161 concentration on its decolorization rates by Fenton processes.

3.5. Influence of H_2O_2/Fe^{2+} molar ratio

In Fenton process, H_2O_2 is catalyzed by ferrous iron to produce hydroxyl radical, HO·. However, too little iron will result in under-utilized H_2O_2, while excessive Fe^{2+} would also scavenge HO· [26]. Therefore, it is important to keep the optimal ratio between H_2O_2 and Fe^{2+} to achieve the best decolorization efficiency of AB161. Theoretically, for organic compounds containing unsaturated azo bond, a transition complex similar to that hydroxylation of trichloroethylene could be assumed [17]. Since the transition state complex has the similar structure which suggests a similar reaction mechanisms and kinetic model, the optimal H_2O_2/Fe^{2+} molar ratio in theory should be 11. This ratio equals the ratio between the two second-order rate constants between H_2O_2 and Fe^{2+} with hydroxyl radical as shown in Eqs. (3) and (4), respectively. It simply reflects a fact that the optimal H_2O_2/Fe^{2+} molar ratio occurs when the scavenging effect by H_2O_2 equal to that by Fe^{2+} (Eq. (13)):

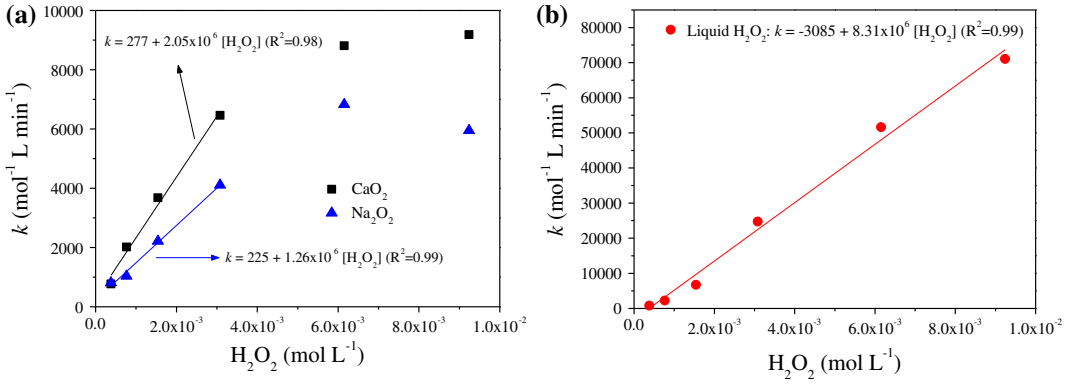

Fig. 4. Linear correlations between the decolorization rate constants vs. H_2O_2 concentration used, obtained during AB161 degradation by Fenton process using (a) CaO_2 and Na_2O_2, and (b) liquid H_2O_2. Initial conditions: [AB161] = 1.0×10^{-4} mol L^{-1}; [Fe^{2+}] = 5.0×10^{-4} mol L^{-1}; pH 2.5.

Table 3
Second-order decolorization rate constants (k) and correlation coefficients (R^2) for each H_2O_2 concentration evaluated to the different H_2O_2 sources

H_2O_2 (mol L^{-1})	$\frac{[H_2O_2]}{[Fe^{2+}]}$	CaO_2		H_2O_2		Na_2O_2	
		k (mol^{-1} L min^{-1})	R^2	k (mol^{-1} L min^{-1})	R^2	k (mol^{-1} L min^{-1})	R^2
0	0	0	–	0	–	0	–
3.8×10^{-4}	0.76	767	0.82	813	0.68	808	0.86
7.6×10^{-4}	1.5	2,018	0.92	2,252	0.82	1,035	0.85
1.5×10^{-3}	3.0	3,682	0.96	6,743	0.96	2,216	0.98
3.1×10^{-3}	6.2	6,460	0.99	24,727	0.97	4,105	0.98
6.2×10^{-3}	12	8,807	0.98	51,604	0.94	6,827	0.98
9.2×10^{-3}	18	9,185	0.98	71,067	0.91	5,950	0.99

Note: Experimental conditions: 5.0×10^{-4} mol L^{-1} Fe^{2+} and pH 2.5.

$$k_3[H_2O_2] = k_4[Fe^{2+}] \quad (13)$$

This optimal condition, however, only applies to organic compound containing unsaturated π bond such as C=C or azo bond (–N=N–) such as AB161 used in this study. If the condition of Eq. (13) is satisfied, neither H_2O_2 nor Fe^{2+} concentration would be overdosed, and the theoretical optimal H_2O_2/Fe^{2+} molar ratio should be expected to be 11. However, the literature documents that the optimal molar ratio of H_2O_2/Fe^{2+} are different for decolorization of different Azo dyes. For example, the optimal molar ratio of H_2O_2/Fe^{2+} was 30:1 and 15:1 at 25°C and pH 3.5 for Fenton oxidation of 2.9×10^{-5} mol L^{-1} Acid Orange 8 and Acid Red 44, respectively [29], and, 100:1 at 30°C and pH 4.0 for 4.7×10^{-5} mol L^{-1} for Fenton oxidation of Direct Blue 15 [30]. To determine the optimal molar ratio of H_2O_2/Fe^{2+} during the decolorization of AB161 in this study, first, the concentration of H_2O_2 was kept constant at 6.2×10^{-3} mol L^{-1}, the amount of Fe^{2+} was varied so that the H_2O_2/Fe^{2+} molar ratio ranged from 12 to 2.5×10^2, as shown in Table 2. Second, Fe^{2+} was maintained constant at 5.0×10^{-4} mol L^{-1}, the amount of H_2O_2 was varied so that the H_2O_2/Fe^{2+} molar ratio ranged from 0.76 to 18 as shown in Table 3. The AB161 decolorization kinetic rate constants at different H_2O_2/Fe^{2+} molar ratios tested are shown in Fig. 5(a) and (b).

Fig. 5(a) and (b) show that the decolorization rate constant at fixed Fe^{2+} concentration of 5.0×10^{-4} mol L^{-1} increases with increasing H_2O_2/Fe^{2+} molar ratio, while it decreases with increasing H_2O_2/Fe^{2+} molar ratio when H_2O_2 concentration was fixed at 6.2×10^{-3} mol L^{-1}. The two curves intersected at about 12, which reasonably agrees with the theoretically predicted value of 11.

To confirm the optimal ratio H_2O_2/Fe^{2+} for the system, a linear correlation was established by plotting the natural logarithm of the decolorization kinetic values vs. the natural logarithm of the H_2O_2/Fe^{2+}

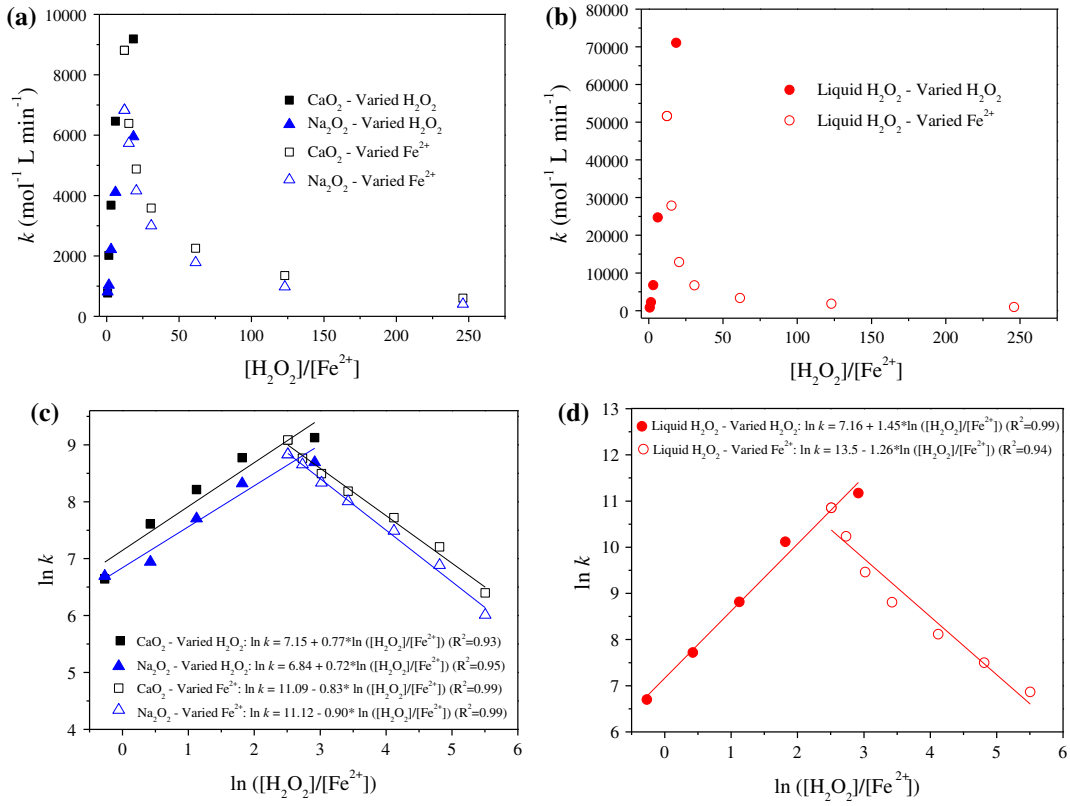

Fig. 5. (a) and (b): direct correlation; and (c) and (d): natural logarithm correlations between the decolorization rate constants vs. H_2O_2/Fe^{2+} molar ratio used, obtained during AB161 degradation by Fenton process, keeping Fe^{2+} constant and ranging H_2O_2, and, vice versa. Initial conditions: [AB161] = 1.0×10^{-4} mol L^{-1}; [Fe^{2+}] = 5.0×10^{-4} mol L^{-1}; [H_2O_2] = 6.2×10^{-3} mol L^{-1} and pH 2.5.

molar ratio (Fig. 5(c) and (d)). Six linear correlation equations were established (Eqs. (14)–(19)). When Fe^{2+} concentration was fixed at 5.0×10^{-4} mol L^{-1}, the oxidation rate constant of AB161 increased with H_2O_2/Fe^{2+} molar ratio to CaO_2, Na_2O_2, and liquid H_2O_2, respectively, as presented by Eqs. (14)–(16):

$$\ln k = 7.15 + 0.77 \times \ln \frac{H_2O_2}{Fe^{2+}} \quad (14)$$

$$\ln k = 6.84 + 0.72 \times \ln \frac{H_2O_2}{Fe^{2+}} \quad (15)$$

$$\ln k = 7.16 + 1.45 \times \ln \frac{H_2O_2}{Fe^{2+}} \quad (16)$$

When H_2O_2 concentration was fixed at 6.2×10^{-3} mol L^{-1}, the oxidation rate constant of AB161 decreases with H_2O_2/Fe^{2+} molar ratio for CaO_2, Na_2O_2, and liquid H_2O_2, respectively, as presented by Eqs. (17)–(19):

$$\ln k = 11.09 - 0.83 \times \ln \frac{H_2O_2}{Fe^{2+}} \quad (17)$$

$$\ln k = 11.12 - 0.90 \times \ln \frac{H_2O_2}{Fe^{2+}} \quad (18)$$

$$\ln k = 13.50 - 1.26 \times \ln \frac{H_2O_2}{Fe^{2+}} \quad (19)$$

When the two equations for each source of hydrogen peroxide were set to equal, e.g. Eq. (14) equals Eq. (17), Eq. (15) equals Eq. (18), Eq. (16) equals Eq. (19), the solution of the two equations gave analytically derived optimal H_2O_2/Fe^{2+} molar ratios of 11.7, 14.0, and 10.4 for CaO_2, liquid H_2O_2, and Na_2O_2, respectively. These optimal ratios were obtained from the intercept of the two straight lines in Fig. 5(c) and (d), respectively. Again, it reasonably agrees with the theoretically predicted value of 11.

Although, the optimal H_2O_2/Fe^{2+} molar ratio was between 10.4 and 14.0, H_2O_2/Fe^{2+} molar ratio of 6.2

was used to evaluate the effects of AB161 concentration on decolorization of AB161 dye by Fenton process. The major reason is that the decolorization rate constants of AB161 increased linearly when the H_2O_2 concentration increased from 3.8×10^{-4} to 3.1×10^{-3} mol L^{-1} due to the limitation of the dissolution of the solid peroxides at concentration higher than 12 g L^{-1} (Fig. 4(a)).

3.6. Influence of AB161 concentration

Initial concentration of dye is an important parameter for practical application. It reflects the effect of organic loading on the decolorization kinetics by Fenton processes. Therefore, it is important to determine how much H_2O_2 and Fe^{2+} are needed to achieve a specific decolorization level. To evaluate this effect, H_2O_2/Fe^{2+} molar ratio and pH were kept at 6.2 and 2.5, respectively. Table 4 presents that the second-order kinetics is the best model at different initial AB161 concentrations with a regression coefficient, R^2, no less than 0.96.

Fig. 6(b) shows the decolorization rates increases exponentially with the H_2O_2/AB161 for CaO_2, Na_2O_2, and liquid H_2O_2. In other words, decolorization rate constants increase as H_2O_2 available per AB161 molecule increases. The natural logarithm of the decolorization kinetics rate constants was plotted against the natural logarithm of H_2O_2/[AB161], linear equations from 20 to 22 can be expressed as follows:

$$\ln k = 1.96 \times \ln \frac{H_2O_2}{AB161} + 2.04 \quad (20)$$

$$\ln k = 4.14 \times \ln \frac{H_2O_2}{AB161} - 4.28 \quad (21)$$

$$\ln k = 1.56 \times \ln \frac{H_2O_2}{AB161} + 3.04 \quad (22)$$

In addition to assess the decolorization kinetics, another way to evaluate the Fenton process is how efficient is the Fenton process according to the available oxidant such as H_2O_2. Decolorization efficiency (η) of AB161 as another dimensionless parameter is used to assess reaction efficiency and is defined in Eq. (23):

$$\eta = \left(\frac{\text{MolesAB161}_{\text{removed}}\ (\text{mol L}^{-1})}{\text{O}_{2\,\text{available}}\ (\text{mol L}^{-1})}\right) = \left(\frac{\text{MolesAB161}_{\text{removed}}\ (\text{mol L}^{-1})}{0.5x[\text{H}_2\text{O}_2]\ (\text{mol L}^{-1})}\right) \quad (23)$$

Fig. 6(a) indicates that decolorization rate constant increases with H_2O_2/AB161. However, Fig. 6(c) shows that the decolorization efficiency (η) decreases with H_2O_2/AB161. It suggests that the higher the dye concentration is the more dye molecules are decolorized. In other words, a higher amount of AB161 is decolorized using less H_2O_2 because increasing dye concentration enhances the interaction between the dye and HO· [31] due to decreased hydroxyl radical scavenging reactions by both H_2O_2 and Fe^{2+} (Eqs. (3) and (4)).

Fig. 6(c) quantitatively correlates the decolorization efficiency, η, with H_2O_2/AB161 molar ratio during AB161 degradation by Fenton process at H_2O_2/Fe^{2+} molar ratio 6.2 using different sources of H_2O_2. The correlation equations (Eqs. (24)–(26)) have a correlation coefficient, R^2, greater than 0.95 for CaO_2, H_2O_2 and Na_2O_2, respectively as follows:

$$\eta = 0.12 - 2.27 \times 10^{-3} \times \ln \frac{H_2O_2}{AB161} \quad (24)$$

$$\eta = 0.13 - 2.81 \times 10^{-3} \times \ln \frac{H_2O_2}{AB161} \quad (25)$$

$$\eta = 0.12 - 2.54 \times 10^{-3} \times \ln \frac{H_2O_2}{AB161} \quad (26)$$

Table 4
Second-order decolorization rate constants (k) and correlation coefficients (R^2) for each AB161 concentration evaluated

AB161 (mol L^{-1})	$\frac{[H_2O_2]}{[AB161]}$	CaO_2		H_2O_2		Na_2O_2	
		k (mol^{-1} L min^{-1})	R^2	k (mol^{-1} L min^{-1})	R^2	k (mol^{-1} L min^{-1})	R^2
1.0×10^{-4}	31	6,460	0.99	24,727	0.97	4,105	0.98
1.2×10^{-4}	26	4,669	0.99	7,860	0.99	3,804	0.99
1.5×10^{-4}	21	3,136	0.99	4,122	0.98	2,354	0.96
1.7×10^{-4}	18	2,199	0.99	2,390	0.97	1,858	0.97

Notes: Experimental conditions: 5.0×10^{-4} mol L^{-1} Fe^{2+}, 3.1×10^{-3} mol L^{-1} H_2O_2 and pH 2.5.

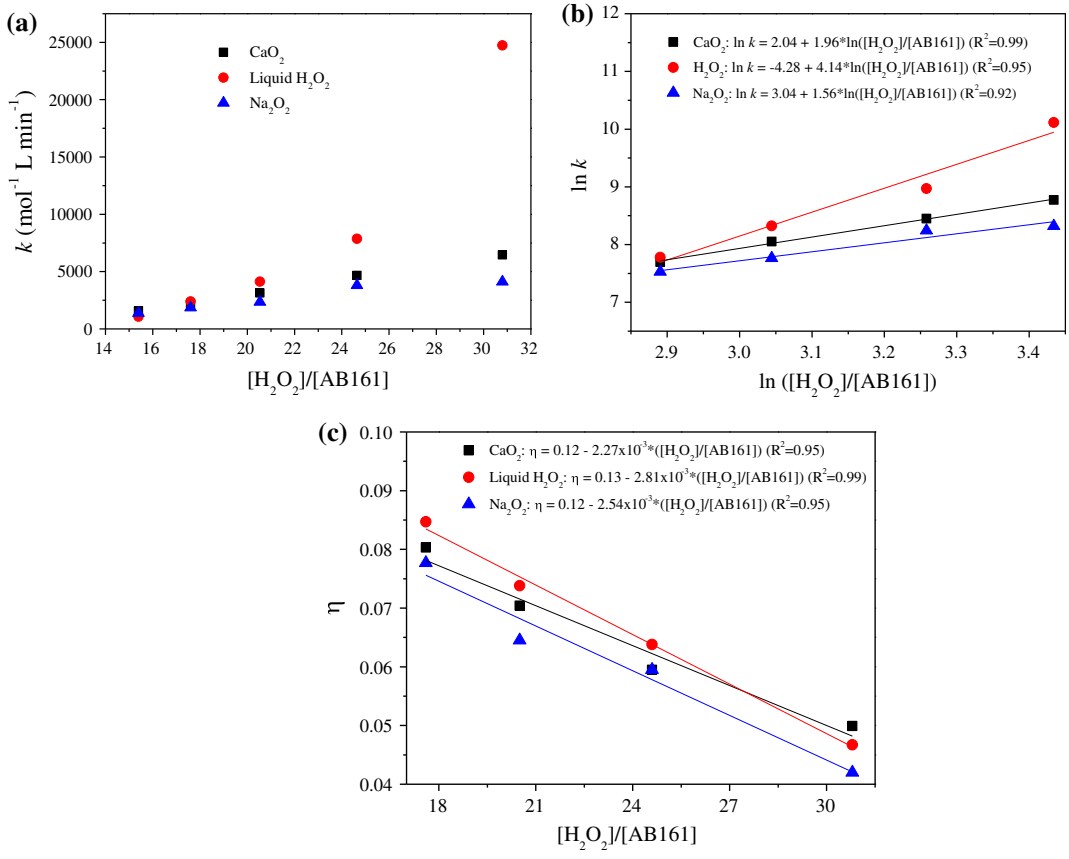

Fig. 6. Correlations between the (a) decolorization rate constants vs. H_2O_2/AB161 M ratio, (b) natural logarithm of decolorization rate constants vs. natural logarithm of H_2O_2/AB161 M ratio, and (c) decolorization efficiency vs. H_2O_2/AB161 M ratio, obtained during AB161 degradation by Fenton process at H_2O_2/Fe^{2+} molar ratio 6.2 using different sources of H_2O_2. Initial conditions: $[Fe^{2+}] = 5.0 \times 10^{-4}$ mol L^{-1}; $[CaO_2]$ and $[Na_2O_2] = 0.30$ and 0.25 g L^{-1}, respectively, of the commercial powders; $[H_2O_2] = 3.1 \times 10^{-3}$ mol L^{-1} of liquid H_2O_2; pH 2.5.

Eqs. (24)–(26) suggest three points: first, decolorization efficiency follows the same quantitative relationship. In other words, solid or liquid peroxide will have the same relationship between the decolorization efficiency and the H_2O_2/AB161 ratio; second, the decolorization efficiency decreases with increasing H_2O_2/AB161 ratio; and third, the maximal decolorization efficiency is about 12% when H_2O_2, Fe^{2+}, and pH were fixed at 3.1×10^{-3}, 5.0×10^{-4} mol L^{-1}; and 2.5, respectively, regardless solid or liquid peroxide is used to produce H_2O_2.

4. Conclusions

It is the first time that the H_2O_2 releasing kinetics from Na_2O_2 for Fenton decolorization of Acid Blue 161 is investigated. About two dozens of correlation equations were established between the second-order decolorization rate constants or efficiency with dimensionless ratios such as H_2O_2/Fe^{2+} or H_2O_2/AB161. It concluded that particle size of the solid peroxides of CaO_2 and Na_2O_2 determines the H_2O_2 releasing rate. The H_2O_2 amount released decreased when pH increased from 3 to 8 because the solid peroxides are strongly alkaline. In addition, hydrogen peroxide has low stability in basic medium where it has greater tendency to decompose into water and oxygen.

The experimental results show that the decolorization kinetics of AB161 followed the second-order kinetics and was significantly affected by concentration of Fe^{2+}, H_2O_2, AB161, and pH. The optimal experimental conditions were obtained as: pH 2.5, $[Fe^{2+}] = 5.0 \times 10^{-4}$ mol L^{-1}, $[CaO_2]$ and $[Na_2O_2] = 0.30$ and 0.25 g L^{-1}, respectively, of the peroxide powders; $[H_2O_2] = 3.1 \times 10^{-3}$ mol L^{-1} of liquid H_2O_2. The best form of H_2O_2 was liquid H_2O_2 due to the reagent costs and implementation simplicity. In addition, the optimal molar ratio H_2O_2/Fe^{2+} of 12 obtained experimentally agreed reasonably with the theoretical predicted value of 11, regardless the solid or liquid

peroxide forms, e.g. CaO_2, Na_2O_2, or liquid H_2O_2. In addition, the decolorization efficiency, η, is also not affected by the form of peroxides and decreases with the H_2O_2/AB161 when H_2O_2, Fe^{2+}, and pH were fixed at 3.1×10^{-3}, 5.0×10^{-4} mol L^{-1}, and 2.5, respectively.

Acknowledgments

This work was supported by Conselho Nacional de Desenvolvimento Científico e Tecnológico–CNPq (Brasil), for the scholarship to A.G. Trovó (Process number: 240990/2012-9); Baltic-American Freedom Foundation (BAFF) for the scholarship to P. Senivs and U. Palmiste.

References

[1] R. Idel-aouad, M. Valiente, A. Yaacoubi, B. Tanouti, M. López-Mesas, Rapid decolourization and mineralization of the azo dye C.I. Acid Red 14 by heterogeneous Fenton reaction, J. Hazard. Mater. 186 (2011) 745–750.

[2] N. Ameta, J. Sharma, S. Sharma, S. Kumar, P.B. Punjabi, Copper modified iron oxide as heterogeneous photo-Fenton reagent for the degradation of coomasie brilliant blue R-250, Indian J. Chem. 51A (2012) 943–948.

[3] S.K.A. Solmaz, A. Birgul, G.E. Ustun, T. Yonar, Colour and COD removal from textile effluent by coagulation and advanced oxidation processes, Color. Technol. 122 (2006) 102–109.

[4] R.O.A. de Lima, A.P. Bazo, D.M.F. Salvadori, C.M. Rech, D.P. Oliveira, G.A. Umbuzeiro, Mutagenic and carcinogenic potential of a textile azo dye processing plant effluent that impacts a drinking water source, Mutat. Res./Genet. Toxicol. Environ. Mutagen. 626 (2007) 53–60.

[5] F.M. Chequer, T.M. Lizier, R. de Felício, M.V. Zanoni, H.M. Debonsi, N.P. Lopes, R. Marcos, D.P. de Oliveira, Analyses of the genotoxic and mutagenic potential of the products formed after the biotransformation of the azo dye Disperse Red 1, Toxicol. In Vitro 25 (2012) 2054–2063.

[6] M.L. Satuf, M.J. Pierrestegui, L. Rossini, R.J. Brandi, O.M. Alfano, Kinetic modeling of azo dyes photocatalytic degradation in aqueous TiO_2 suspensions. Toxicity and biodegradability evaluation, Catal. Today 161 (2011) 121–126.

[7] Y.-Y. Lau, Y.-S. Wong, T.-T. Teng, N. Morad, M. Rafatullah, S.-A. Ong, Coagulation–flocculation of azo dye Acid Orange 7 with green refined laterite soil, Chem. Eng. J. 246 (2014) 383–390.

[8] D. Morshedi, Z. Mohammadi, M.M.A. Boojar, F. Aliakbari, Using protein nanofibrils to remove azo dyes from aqueous solution by the coagulation process, Colloids Surf., B 112 (2013) 245–254.

[9] M.A. Kamboh, A.A. Bhatti, I.B. Solangi, S.T.H. Sherazi, S. Memon, Adsorption of direct black-38 azo dye on *p-tert*-butylcalix[6]arene immobilized material, Arab. J. Chem. 7 (2014) 125–131.

[10] W.Z. Tang, R.Z. Chen, Decolorization kinetics and mechanisms of commercial dyes by H_2O_2/iron powder system, Chemosphere 32 (1996) 947–958.

[11] N.M. Ghazi, A.A. Lastra, M.J. Watts, Hydroxyl radical (OH) scavenging in young and mature landfill leachates, Water Res. 56 (2014) 148–155.

[12] A.N. Soon, B.H. Hameed, Heterogeneous catalytic treatment of synthetic dyes in aqueous media using Fenton and photo-assisted Fenton process, Desalination 269 (2011) 1–16.

[13] C. Walling, Fenton's reagent revisited, Acc. Chem. Res. 8 (1975) 125–131.

[14] D. Prato-Garcia, G. Buitrón, Improvement of the robustness of solar photo-Fenton processes using chemometric techniques for the decolorization of azo dye mixtures, J. Environ. Manage. 131 (2013) 66–73.

[15] N. Ertugay, F.N. Acar, Removal of COD and color from Direct Blue 71 azo dye wastewater by Fenton's oxidation: Kinetic study, Arab. J. Chem. 2 (2013) 1–6.

[16] M.M. Ghoneim, H.S. Él-Desoky, N.M. Zidan, Electro-Fenton oxidation of Sunset Yellow FCF azo-dye in aqueous solutions, Desalination 274 (2011) 22–30.

[17] W.Z. Tang, Physicochemical Treatment of Hazardous Wastes, Lewis Publishers, Boca Raton, 2004.

[18] A.-C. Ndjou'ou, D. Cassidy, Surfactant production accompanying the modified Fenton oxidation of hydrocarbons in soil, J. Hazard. Mater. 65 (2006) 1610–1615.

[19] B.W. Bogan, V. Trbovic, J.R. Paterek, Inclusion of vegetable oils in Fenton's chemistry for remediation of PAH-contaminated soils, Chemosphere 50 (2003) 15–21.

[20] A. Northup, D. Cassidy, Calcium peroxide (CaO_2) for use in modified Fenton chemistry, J. Hazard. Mater. 152 (2008) 1164–1170.

[21] R.F.P. Nogueira, M.C. Oliveira, W.C. Paterlini, Simple and fast spectrophotometric determination of H_2O_2 in photo-Fenton reactions using metavanadate, Talanta 66 (2005) 86–91.

[22] I.L. Mattos, K.A. Shiraishi, A.D. Braz, J.R. Fernandes, Peróxido de hidrogênio: Importância e determinação (Importance and determination of hydrogen peroxide), Quím. Nova 26 (2003) 373–380.

[23] J.E. Girard, Principles of Environmental Chemistry, second ed., LTC, Rio de Janeiro, 2013.

[24] M.S. Lucas, J.A. Peres, Decolorization of the azo dye Reactive Black 5 by Fenton and photo-Fenton oxidation, Dyes Pigm. 71 (2006) 236–244.

[25] F. Fu, Q. Wang, B. Tang, Effective degradation of C.I. Acid Red 73 by advanced Fenton process, J. Hazard. Mater. 174 (2010) 17–22.

[26] S.-P. Sun, C.-J. Li, J.-H. Sun, S.-H. Shi, M.-H. Fan, Q. Zhou, Decolorization of an azo dye Orange G in aqueous solution by Fenton oxidation process: Effect of system parameters and kinetic study, J. Hazard. Mater. 161 (2009) 1052–1057.

[27] F. Emami, A.R. Tehrani-Bagha, K. Gharanjig, F.M. Menger, Kinetic study of the factors controlling Fenton-promoted destruction of a non-biodegradable dye, Desalination 257 (2010) 124–128.

[28] X.R. Xu, Z.Y. Zhao, X.Y. Li, J.D. Gu, Chemical oxidative degradation of methyl *tert*-butyl ether in aqueous solution by Fenton´s reagent, Chemosphere 55 (2004) 73–79.

[29] S. Tunç, O. Duman, T. Gürkan, Monitoring the decolorization of Acid Orange 8 and Acid Red 44 from aqueous solution using Fenton's reagents by online spectrophotometric method: Effect of operation parameteres and kinetic study, Ind. Eng. Chem. Res. 52 (2013) 1414–1425.
[30] J.-H. Sun, S.-H. Shi, Y.-F. Lee, S.-P. Sun, Fenton oxidative decolorization of the azo dye Direct Blue 15 in aqueous solution, Chem. Eng. J. 155 (2009) 680–683.
[31] Y. Wu, S. Zhou, F. Qin, K. Zheng, X. Ye, Modeling the oxidation kinetics of Fenton's process on the degradation of humic acid, J. Hazard. Mater. 179 (2010) 533–539.